



Numerical Solutions for Flow of an Oldroyd Fluid Confined between Coaxial Rotating Disks

R. K. Bhatnagar and M. G. N. Perera

Citation: *Journal of Rheology* (1978-present) **26**, 19 (1982); doi: 10.1122/1.549658

View online: <http://dx.doi.org/10.1122/1.549658>

View Table of Contents: <http://scitation.aip.org/content/sor/journal/jor2/26/1?ver=pdfcov>

Published by the [The Society of Rheology](#)

Articles you may be interested in

[The matching of polymer solution fast filament stretching, relaxation, and break up experimental results with 1D and 2D numerical viscoelastic simulation](#)

J. Rheol. **56**, 1491 (2012); 10.1122/1.4749828

[ReEntrant Corner Flows of OldroydB fluids in the Natural Stress Basis](#)

AIP Conf. Proc. **1027**, 285 (2008); 10.1063/1.2964665

[Vortex Shedding in Confined Swirling Flows of Polymer Solutions with a Partially Rotating Disc](#)

AIP Conf. Proc. **1027**, 222 (2008); 10.1063/1.2964642

[HighShear Viscometry with a Rotational ParallelDisk Device](#)

J. Rheol. **29**, 209 (1985); 10.1122/1.549828

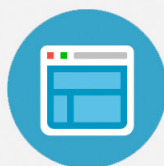
[Lubrication Flows in Viscoelastic Liquids. I. Squeezing Flow between Approaching Parallel Rigid Planes](#)

J. Rheol. **26**, 1 (1982); 10.1122/1.549657



Re-register for Table of Content Alerts

Create a profile.



Sign up today!



Numerical Solutions for Flow of an Oldroyd Fluid Confined between Coaxial Rotating Disks

R. K. BHATNAGAR,* *Institute of Mathematics, Statistics and
Computer Science, Universidade Estadual de Campinas,
Campinas (SP) Brazil*, and M. G. N. PERERA,† *Department of
Chemical Engineering, University of Dortmund, Dortmund, West
Germany*

Synopsis

The problem of flow of an elasticoviscous fluid characterized by a four-constant Oldroyd model is treated when such a fluid is confined between a pair of infinite coaxial parallel disks. The governing system of nonlinear coupled differential equations for the stresses and the velocity field is expressed by the corresponding finite difference analogs and solved by using the SOR method. For the case of one disk held at rest, the solutions are provided for Reynolds numbers 10 and 100, while for the case of counterrotations of the disks, they are also provided for the intermediate value of 20. The graphical representations of the velocity functions bring out some very interesting differences in the behavior of a Newtonian, slightly elastic and an elastic liquid.

INTRODUCTION

Recently, Bhatnagar and Zago¹ provided solutions for the flow of a viscoelastic fluid of the Rivlin–Ericksen type confined between a pair of coaxial rotating disks by integrating the governing equations numerically. The finite difference analogs of the governing nonlinear ordinary differential equations were obtained, and the resulting system was solved using the point-successive overrelaxation (SOR) method, under the appropriate boundary conditions of the problem. In the work of Bhatnagar and Zago,¹ two cases of interest were treated,

* Presently visiting professor in the Polymer Engineering Program, University of Tennessee, Knoxville, Tennessee.

† Present address: Department of Mechanical Engineering, Twente University of Technology, Enschede, The Netherlands.

© 1982 by The Society of Rheology, Inc. Published by John Wiley & Sons, Inc.
Journal of Rheology, 26(1), 19–41 (1982) CCC 0148-6055/82/010019-23\$02.30

namely, (1) where one disk is held at rest while the other rotates with a constant angular velocity, and (2) where both the disks rotate with same constant angular velocity but in opposite directions. Typical examples for flow have been given for the Reynolds number Re in the range $10 < Re < 100$ and the results have been compared with those for a Newtonian fluid.²⁻⁹ There have also been studies reported in the literature for flow of non-Newtonian liquids between rotating disks¹⁰⁻¹² where use of either perturbation techniques or numerical procedures was made.

The purpose of the present investigation is to discuss the same problem as in ref. 1 but for an elasticoviscous fluid characterized by a four-constant Oldroyd model. It may be noted that this model is superior to the Rivlin-Ericksen model used for the same problem in ref. 1.

The equations of state relating the stress tensor \mathbf{S}_{ik} and the rate-of-strain tensor $\mathbf{E}_{ik} = (1/2)(\mathbf{u}_{k,i} + \mathbf{u}_{i,k})$ for an idealized incompressible elasticoviscous fluid as given by Oldroyd¹³ have the following form:

$$\mathbf{S}_{ik} = \mathbf{T}_{ik} - P\mathbf{g}_{ik}, \quad (1)$$

$$\mathbf{T}^{ik} + \lambda_1 \frac{\delta \mathbf{T}^{ik}}{\delta t} + \mu_0 \mathbf{T}_j^j \mathbf{E}^{ik} = 2\eta_0 \left(\mathbf{E}^{ik} + \lambda_2 \frac{\delta \mathbf{E}^{ik}}{\delta t} \right), \quad (2)$$

where \mathbf{u}_i denotes the velocity vector, \mathbf{g}_{ik} the metric tensor, \mathbf{T}_{ik} the part of the stress tensor related to change of shape of a material element, and P an isotropic pressure; η_0 represents the viscosity of the fluid and λ_1 , λ_2 , and μ_0 are constants having dimensions of time.

If \mathbf{B}^{ik} is any contravariant tensor, then the convected time derivative $\delta/\delta t$ in Eq. (2) is defined as

$$\frac{\delta}{\delta t} \mathbf{B}^{ik} = \frac{\partial \mathbf{B}^{ik}}{\partial t} + \mathbf{u}^j \mathbf{B}_j^k + \Omega_m^i \mathbf{B}^{mk} - \mathbf{E}_m^i \mathbf{B}^{mk} - \mathbf{E}_m^k \mathbf{B}^{im}, \quad (3)$$

where $\Omega_{ik} = (1/2)(\mathbf{u}_{k,i} - \mathbf{u}_{i,k})$ is the vorticity tensor.

It is shown by Oldroyd¹³ that if the equations of state [Eqs. (1) and (2)] are to represent certain important non-Newtonian flow properties over the whole range of rates of shear, then λ_1 , λ_2 , and μ_0 must satisfy

the relations

$$\lambda_1 \geq \lambda_2 \geq \frac{1}{9} \lambda_1 > 0, \quad \mu_0 > 0.$$

In the present investigation we shall be considering the same two cases of the boundary conditions as in ref. 1.

EQUATIONS OF MOTION

Consider the steady motion of a mass of elasticoviscous fluid, which is characterized by the rheological equations of state [Eqs. (1) and (2)] and is confined between two infinite coaxial parallel disks. Choosing a cylindrical polar coordinate system (R, θ, Z) , let the lower disk in the plane $Z = 0$ rotate with an angular velocity Ω and the upper disk located in the plane $Z = d$ rotate with an angular velocity $\alpha\Omega$. Let $U, V,$ and W represent the physical components of the velocity vector in this system of coordinates.

For the above motion, the boundary conditions can then be written as

$$\begin{aligned} U = W = 0, \quad V = R\Omega \quad \text{on } Z = 0, \\ U = W = 0, \quad V = R\alpha\Omega \quad \text{on } Z = d. \end{aligned} \tag{4}$$

In order to derive the governing system of equations, we write the equations of continuity and momentum in cylindrical coordinate system. The momentum equations contain components of stress which are given by Eqs. (1)–(3) written out in cylindrical coordinate system.

Before proceeding further, we first reduce these ten equations, viz., six for the stress components and four as equations of momentum and continuity, to their nondimensional form using the following substitutions:

$$\begin{aligned} R = dr, \quad Z = dz, \quad U = d\Omega u \quad V = d\Omega v, \\ W = d\Omega w, \quad T_{ik} = \eta_0 \Omega t_{ik}, \quad P = \rho \Omega^2 d^2 p, \end{aligned} \tag{5}$$

where t_{ik} represents the physical components of the partial stress tensor.

As is clear, the above set of equations after nondimensionalization will involve the Reynolds number Re defined as $Re = d^2 \Omega \rho / \eta_0$ and other three positive parameters $\sigma = (\lambda_2 / \lambda_1)$, $\epsilon = (\mu_0 / \lambda_1)$, and $S = \lambda_1 \Omega$. It may be noted that σ and ϵ represent dimensionless physical constants of the material, whereas S , the Weissenberg number, characterizes the memory of the elasticoviscous fluid under consideration.

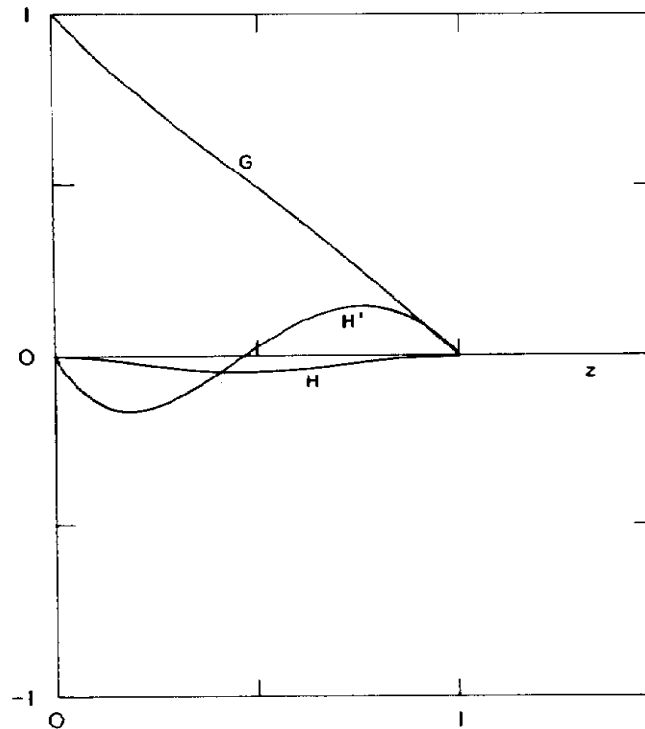


Fig. 1. Velocity functions G , H , and H' for a Newtonian fluid and non-Newtonian fluid with $\Delta z = 0.02$, $\alpha = 0$, $\text{Re} = 10$, $\lambda_1 = 0.10$, $\lambda_2 = 0.02$, $\mu_0 = 1.00$.

In view of Eq. (5), the nondimensionalized boundary conditions become

$$\begin{aligned} u = 0, \quad v = r, \quad w = 0 \quad \text{on } z = 0, \\ v = 0, \quad v = \alpha r, \quad w = 0 \quad \text{on } z = d. \end{aligned} \quad (6)$$

In order to solve the set of ten nonlinear partial differential equations for the problem under consideration, we first transform them to a set of ordinary nonlinear differential equations with the help of the following similarity transformations:

$$\begin{aligned} u = -\frac{1}{2} r H'(z), \quad v = r G(z), \quad w = H(z); \\ t_{rr} = F_1(z) + r^2 F_2(z), \quad t_{\theta\theta} = F_1(z) + r^2 G_2(z), \\ t_{zz} = H_1(z) + r^2 H_2(z), \quad t_{\theta z} = r K_1(z), \\ t_{rz} = r L_1(z), \quad t_{r\theta} = r^2 M_1(z), \end{aligned} \quad (7)$$

$$(8)$$

where a prime denotes differentiation with respect to z .

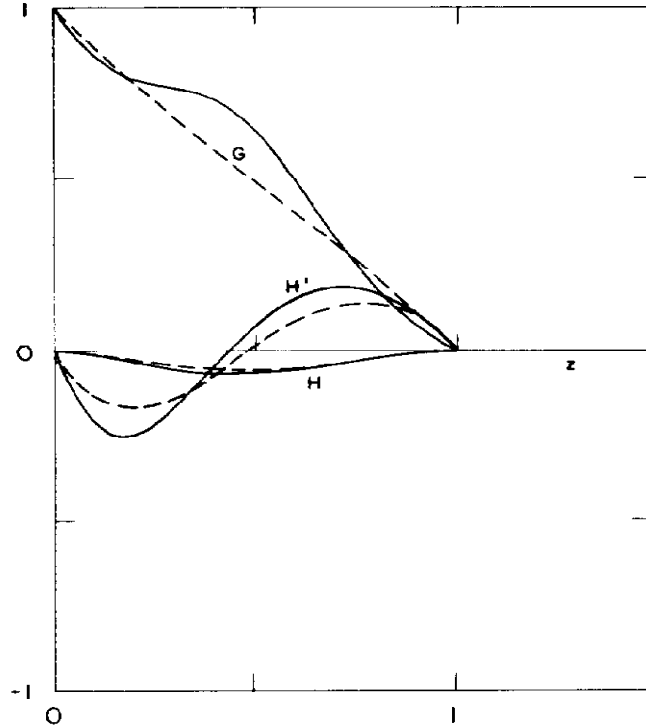


Fig. 2. Comparison of functions G , H , and H' for an elastic fluid (—) where $\lambda_1 = 2.00$, $\lambda_2 = 0.33$, $\mu_0 = 0.50$ with those for a slightly elastic fluid (---) where $\lambda_1 = 0.10$, $\lambda_2 = 0.02$, $\mu_0 = 1.00$; $\Delta z = 0.02$, $\alpha = 0$, and $Re = 10$.

With the choice of u , v , and w , as in Eq. (7), it can be easily verified that the equation of continuity is identically satisfied.

Reduced Form of the Stress Equations

Substituting the expressions for t_{rr} , $t_{\theta\theta}$, etc., from Eq. (8) into the stress equations, we get the following set of ordinary differential equations satisfied by the functions F_1 , F_2 , G_2 , H_1 , H_2 , K_1 , L_1 , and M_1 :

$$F_1 + S(HF'_1 + H'F_1) - \frac{1}{2} H' \epsilon S(2F_1 + H_1) = -H' - \sigma S(HM + H'^2), \quad (9)$$

$$F_2 + S(HF'_2 + ML_1) - \frac{1}{2} H' \epsilon S(F_2 + G_2 + H_2) = -\frac{1}{2} \sigma SM^2, \quad (10)$$

$$G_2 + S(HG_2 - 2G'K_1) - \frac{1}{2} H' \epsilon S(F_2 + G_2 + H_2) = -2\sigma SG'^2, \quad (11)$$

$$H_1 + S(HH'_1 - 2H'H_1) + H' \epsilon S(2F_1 + H_1) = 2H' + \sigma S(2Hm - 4H'^2), \quad (12)$$

$$H_2 + S(HH'_2 - 3H'H_2) + H' \epsilon S(F_2 + G_2 + H_2) = 0, \quad (13)$$

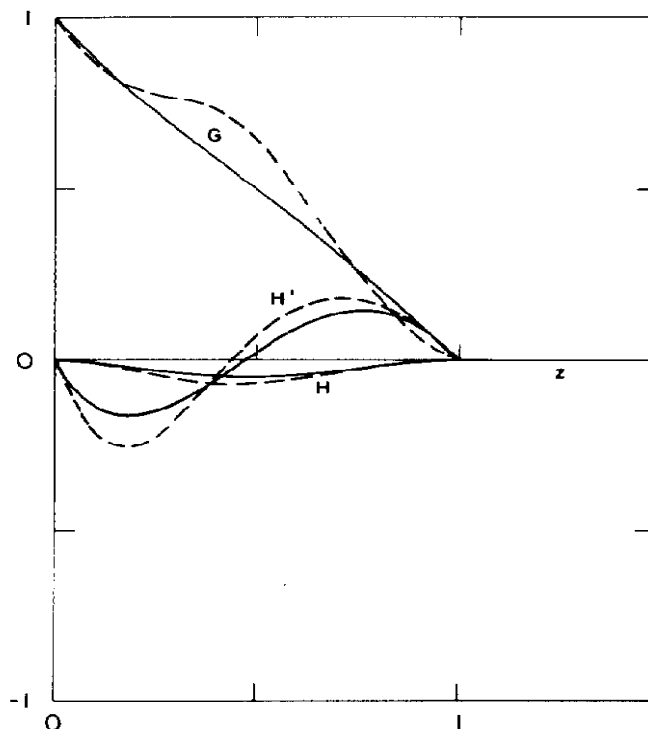


Fig. 3. Comparison of velocity functions G , H , and H' for a Newtonian fluid (—) with those for an elastic fluid (---) where $\lambda_1 = 2.00$, $\lambda_2 = 0.33$, $\mu_0 = 0.50$; $\Delta z = 0.02$, $\alpha = 0$, $\text{Re} = 10$.

$$K_1 + S(HK'_1 - G'H_1) + \frac{1}{2} G' \epsilon S(2F_1 + H_1) = G' + \sigma S(HG'' - 2H'G'), \quad (14)$$

$$L_1 + S(HL'_1 - H'L_1 + \frac{1}{2} MH_1) - \frac{1}{4} M \epsilon S(2F_1 + H_1) = -\frac{1}{2} M + \frac{\sigma S}{2} (3H'M - HM'), \quad (15)$$

and

$$M_1 + S(HM'_1 + \frac{1}{2} MK_1 - G'L_1) = \sigma SMG', \quad (16)$$

where

$$H'' = M. \quad (17)$$

Reduced Form of the Equations of Motion

We now make use of the expressions in Eqs. (7) and (8) to reduce the equations of motion to more suitable forms.

It can be easily verified that the equation of motion in the θ directions transforms to

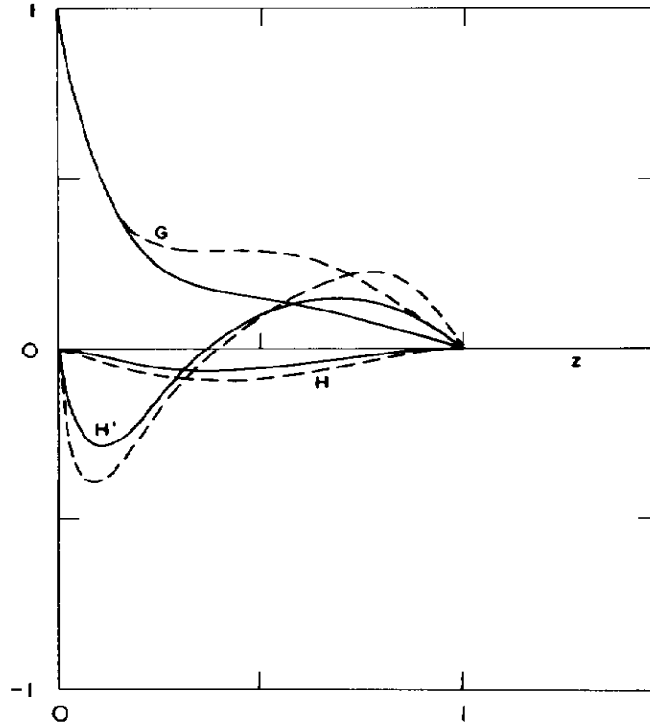


Fig. 4. Comparison of velocity functions G , H , and H' for a Newtonian fluid (---) with those for a slightly elastic non-Newtonian fluid (—) where $\lambda_1 = 0.50$, $\lambda_2 = 0.08$, $\mu_0 = 2.00$; $\Delta z = 0.02$, $\alpha = 0$, $Re = 100$.

$$Re(HG' - H'G) = 4M_1 + K'_1. \tag{18}$$

Eliminating the pressure p between the equations of motion in the radial and axial directions and making use of Eqs. (7) and (8) in the resulting equation, we get, after making simplifications,

$$Re(HM' + 4GG') = 2(G'_2 - 3F'_2) + 4H'_2 - 2L''_1. \tag{19}$$

The associated boundary conditions for Eqs. (18) and (19) are

$$G(0) = 1, \quad G(1) = \alpha, \quad H(0) = H'(0) = 0, \quad H(1) = H'(1) = 0. \tag{20}$$

Now if we write

$$\begin{aligned} F_1 &= -H' + \bar{F}_1, & F_2 &= \bar{F}_2, & G_2 &= \bar{G}_2, \\ H_1 &= 2H' + \bar{H}_1, & H_2 &= \bar{H}_2, & K_1 &= G' + \bar{K}_1, \\ L_1 &= -\frac{1}{2}M + \bar{L}_1, & M_1 &= \bar{M}_1, \end{aligned} \tag{21}$$

then Eqs. (18) and (19) reduce to the forms,

$$G'' + Re(H'G - HG') = -(4\bar{M}_1 + \bar{K}'_1), \tag{22}$$

and

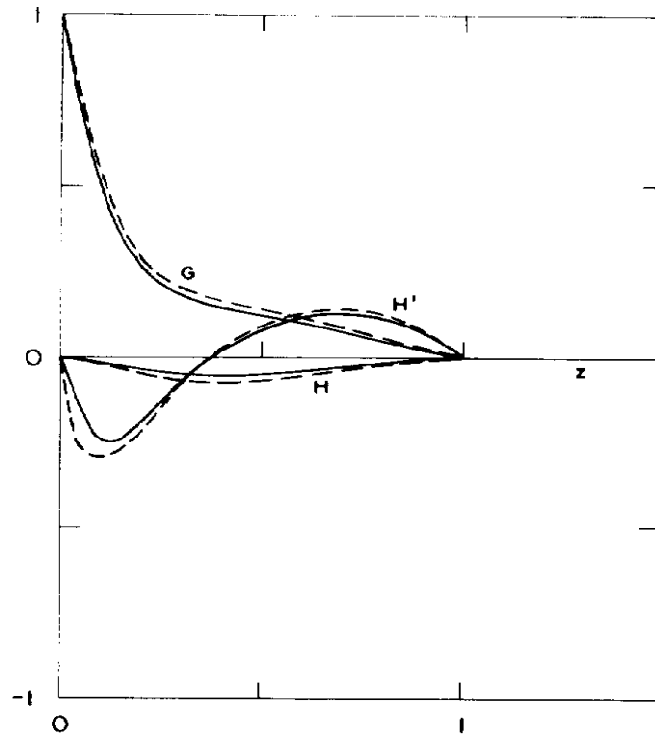


Fig. 5. Comparison between velocity functions G , H , and H' for a non-Newtonian slightly elastic fluid (---) having $\lambda_1 = 0.50$, $\lambda_2 = 0.08$, $\mu_0 = 2.00$ with those of an elastic fluid (—) having $\lambda_1 = 1.50$, $\lambda_2 = 0.25$, $\mu_0 = 0.67$; $\Delta z = 0.02$, $\alpha = 0$, $\text{Re} = 100$.

$$M'' - \text{Re}(HM' + 4GG') = 2\bar{L}_1'' - 2(\bar{G}'_2 - 3\bar{F}'_2) - 4\bar{H}'_2. \quad (23)$$

The equations satisfied by K_1 and L_1 can be deduced easily with the help of Eqs. (14) and (15). If $S = 0$, the above set of Eqs. (22) and (23) reduces to the well-known equations for the flow of a classical viscous fluid.

Using the conditions on the velocity functions as given in Eq. (20) in conjunction with the Eqs. (9)–(16), we can easily write the values of the functions F_1 , F_2 , G_2 , H_1 , H_2 , K_1 , L_1 , and M_1 at the two disks. Thus, it can be easily checked that

$$\begin{aligned} F_1(0) &= 0, & F_2(0) &= \frac{1}{2} S(1 - \sigma)[M(0)]^2, \\ G_2(0) &= 2S(1 - \sigma)[G'(0)]^2, & H_1(0) &= 0, & H_2(0) &= 0, \\ K_1(0) &= G'(0), & L_1(0) &= -\frac{1}{2} M(0), \\ M_1(0) &= S(\sigma - 1)M(0)G'(0); \end{aligned} \quad (24)$$

and

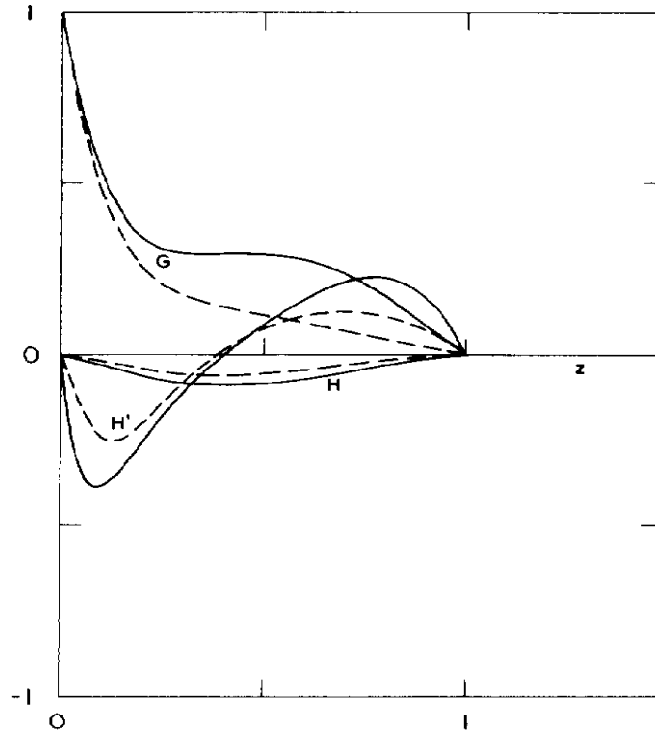


Fig. 6. Comparison of velocity components for a Newtonian fluid (—) with those of an elastic fluid (---) having $\lambda_1 = 1.5$, $\lambda_2 = 0.25$, $\mu_0 = 0.67$; $\Delta z = 0.02$, $\alpha = 0$, $Re = 100$.

$$\begin{aligned}
 F_1(1) &= 0, & F_2(1) &= \frac{1}{2} S(1 - \sigma)[M(1)]^2, \\
 G_2(1) &= 2S(1 - \sigma)[G'(1)]^2, & H_1(1) &= 0, & H_2(1) &= 0, \\
 K_1(1) &= G'(1), & L_1(1) &= -\frac{1}{2} M(1), \\
 M_1(1) &= S(\sigma - 1)M(1)G'(1). & & & & (25)
 \end{aligned}$$

In the next section we describe the numerical procedure adopted to solve the system of coupled ordinary nonlinear differential Eqs. (9)–(17), (22), and (23) using the boundary conditions in Eq. (20) and the conditions on the stress functions given by Eqs. (24) and (25).

NUMERICAL PROCEDURE

The system of Eqs. (9)–(17), (22), and (23) are solved using finite difference methods. The dimensionless distance z between the two disks is divided into 50 equal parts. The detailed description of the finite difference approximations of the Eqs. (17), (22), and (23) have been already given in ref. 1 so that we shall not discuss the method of obtaining their finite difference analogs here.

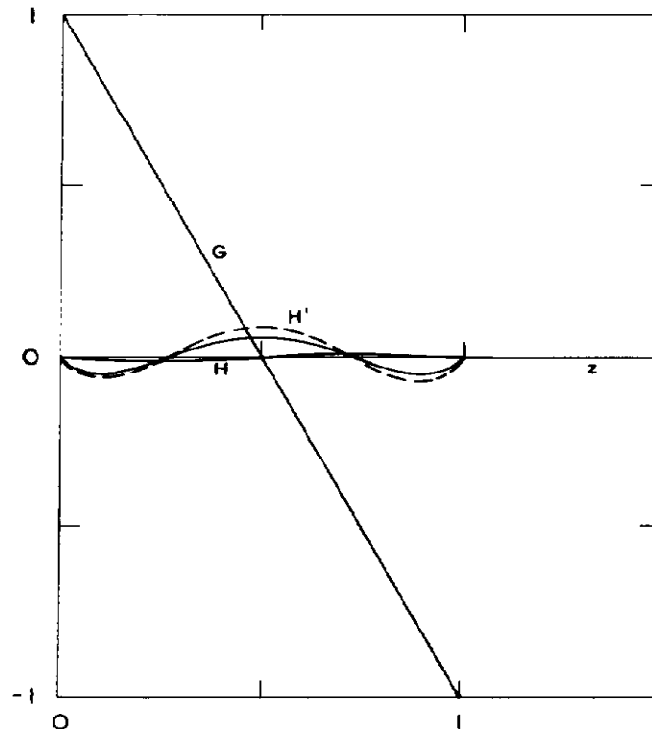


Fig. 7. Comparison of velocity functions for a Newtonian fluid (---) with those of a slightly elastic non-Newtonian fluid (—) having $\lambda_1 = 0.20$, $\lambda_2 = 0.03$, $\mu_0 = 5.00$; $\Delta z = 0.02$, $\alpha = -1.0$, $Re = 10$.

The Solution of Stress Equations

It is now our purpose to discuss the method of obtaining the finite difference analogs of the equations for stress components Eqs. (9)–(16) which constitute a set of eight first-order coupled differential equations. We solve these equations as a set of simultaneous equations.

In solving matrix equations of the form $AX = B$ by iterative methods, it is necessary for the local convergence of the iterative scheme and helpful for global convergence to have each iterative matrix diagonally dominant,^{14–16} especially when coupled sets of equations are involved. To achieve this, a sort of upwind differencing scheme is employed to discretize the stress Eq. (16). To show the details of this procedure, we first write Eqs. (9)–(16) as a single equation in the form

$$SH \frac{\partial}{\partial z} P_i + C_{ii}P_i + \sum_{\substack{j=1 \\ j \neq i}}^8 C_{ij}P_j = X_i, \quad i = 1, 2, \dots, 8, \quad (26)$$

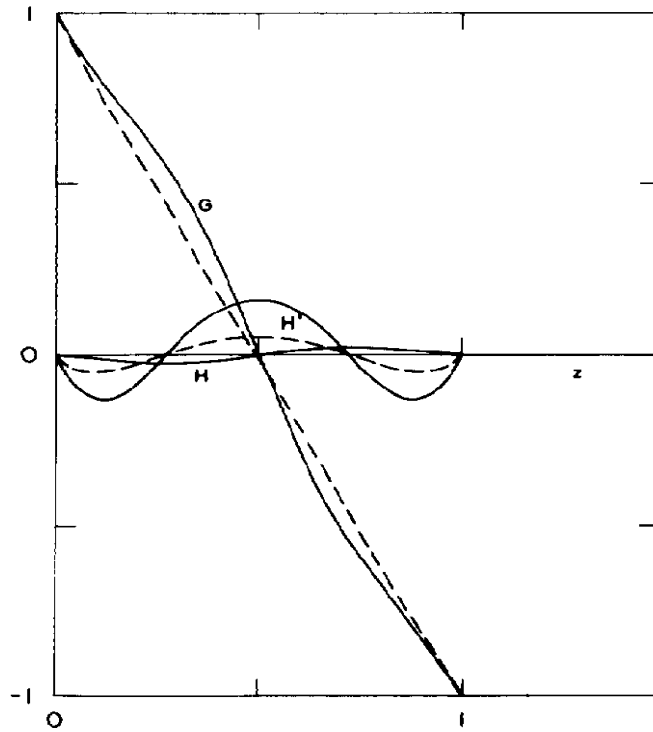


Fig. 8. Comparison of velocity function for an elastic non-Newtonian fluid (—) having $\lambda_1 = 1.25, \lambda_2 = 0.21, \mu_0 = 0.80$ with a slightly elastic non-Newtonian (---) fluid with $\lambda_1 = 0.20, \lambda_2 = 0.03, \mu_0 = 5.00; \Delta z = 0.02, \alpha = -1.0, Re = 10$.

where P_i represents the components of stress. It may be noted that in Eq. (26) summation is not implied for repeated indices except where indicated. Furthermore, S is taken to be greater than 0. The derivative $\partial/\partial z$ is discretized using one-sided differences, backward or forward depending on the signs of C_{ii} and H . We note that no summation is implied in the repeated indices in C_{ii} .

Let k be a grid point corresponding to a point z and $k + 1, k - 1$ the neighboring grid points on either side of k .

If $H > 0, C_{ii} > 0$ at k , then we write

$$\partial P_i / \partial z = (P_i^k - P_i^{k-1}) / \Delta z, \tag{27}$$

so that the discretized form of Eq. (26) is

$$SH(P_i^k - P_i^{k-1}) / \Delta z + C_{ii} P_i^k = X_i^k - \sum_{\substack{j=1 \\ j \neq i}}^8 C_{ij}^k P_j^k, \tag{28}$$

giving

$$P_i^k = \left(\frac{SH}{\Delta z} + C_{ii} \right)^{-1} \left(X_i^k - \sum_{\substack{j=1 \\ j \neq i}}^8 C_{ij}^k P_j^k + P_i^{k-1} \frac{SH}{\Delta z} \right), \tag{29}$$

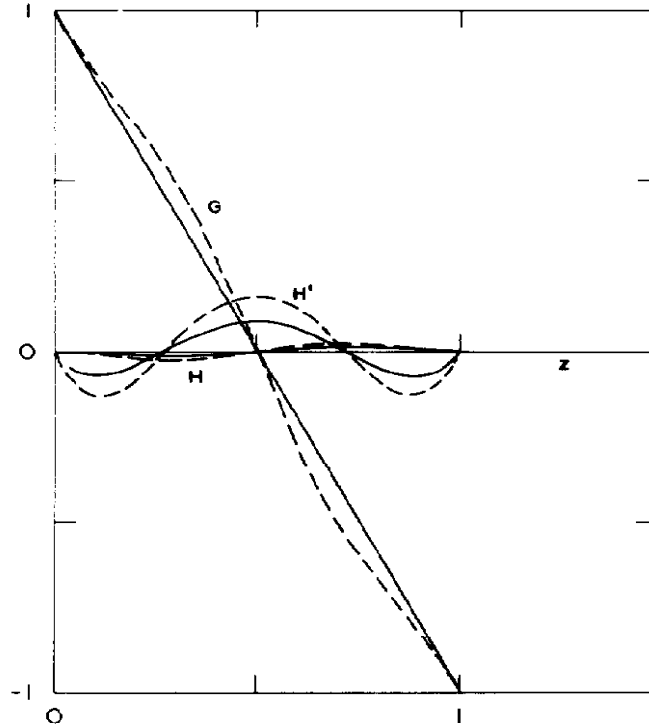


Fig. 9. Comparison of velocity functions for a Newtonian fluid (—) with those of an elastic fluid (---) having $\lambda_1 = 1.25$, $\lambda_2 = 0.21$, $\mu_0 = 0.80$; $\Delta z = 0.02$, $\alpha = -1.0$, $\text{Re} = 10$.

Since H and C_{ii} are both greater than 0,

$$P_i^k = \left(\frac{S|H|}{\Delta z} + |C_{ii}| \right)^{-1} \left(X_i^k - \sum_{\substack{j=1 \\ j \neq i}}^8 C_{ij}^k P_j^k + P_i^{k-1} \frac{SH}{\Delta z} \right). \quad (30)$$

It is easily seen that the iterative matrix corresponding to Eq. (30) is diagonally dominant.

If $H < 0$, $C_{ii} > 0$, we take

$$\partial P_i / \partial z = (P_i^{k+1} - P_i^k) / \Delta z, \quad (31)$$

which gives

$$P_i^k = \left(\frac{S|H|}{\Delta z} + |C_{ii}| \right)^{-1} \left(X_i^k - \sum_{\substack{j=1 \\ j \neq i}}^8 C_{ij}^k P_j^k - P_i^{k+1} \frac{SH}{\Delta z} \right). \quad (32)$$

If $H > 0$, $C_{ii} < 0$, we write

$$\partial P_i / \partial z = (P_i^{k+1} - P_i^k) / \Delta z$$

giving

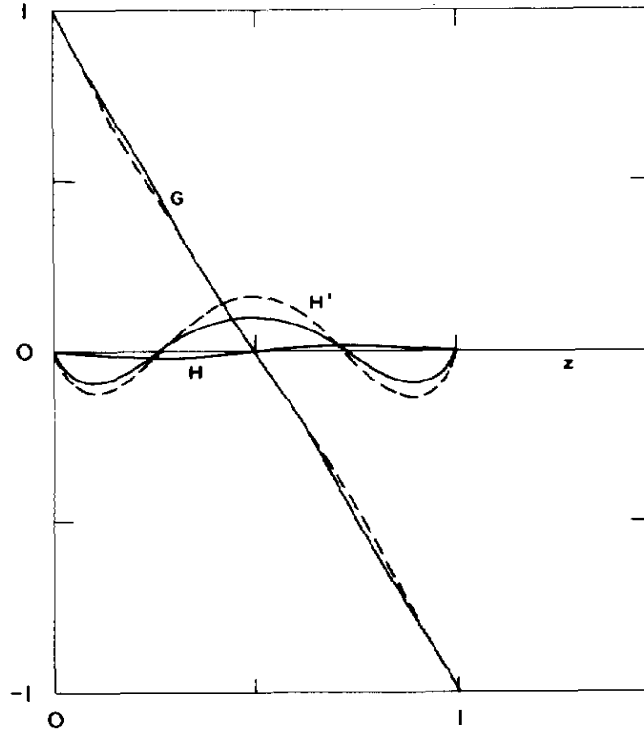


Fig. 10. Comparison of velocity functions for a slightly elastic non-Newtonian fluid (—) having $\lambda_1 = 0.20$, $\lambda_2 = 0.03$, $\mu_0 = 5.00$ with those of a Newtonian fluid (---); $\Delta z = 0.02$, $\alpha = -1.0$, $Re = 20$.

$$P_i^k = - \left(\frac{S|H|}{\Delta z} + |C_{ii}| \right)^{-1} \left(X_i^k - \sum_{\substack{j=1 \\ j \neq i}}^8 C_{ij}^k P_j^k - P_i^{k+1} \frac{SH}{\Delta z} \right). \quad (33)$$

Lastly, if $H < 0$, $C_{ii} < 0$, we write

$$\partial P_i / \partial z = (P_i^k - P_i^{k-1}) / \Delta z, \quad (34)$$

so that

$$P_i^k = - \left(\frac{S|H|}{\Delta z} + |C_{ii}| \right)^{-1} \left(X_i^k - \sum_{\substack{j=1 \\ j \neq i}}^8 C_{ij}^k P_j^k + P_i^{k-1} \frac{SH}{\Delta z} \right). \quad (35)$$

To form a single equation for P_i at the grid point k from the Eqs. (30), (32), (33), and (35), we introduce three integers c , HMAX, and HMIN such that

$$\begin{aligned} C_{ii} > 0 &\text{ implies } c = 0, \\ C_{ii} < 0 &\text{ implies } c = 1, \\ H > 0 &\text{ implies HMAX} = 1, \text{ HMIN} = 0, \end{aligned}$$

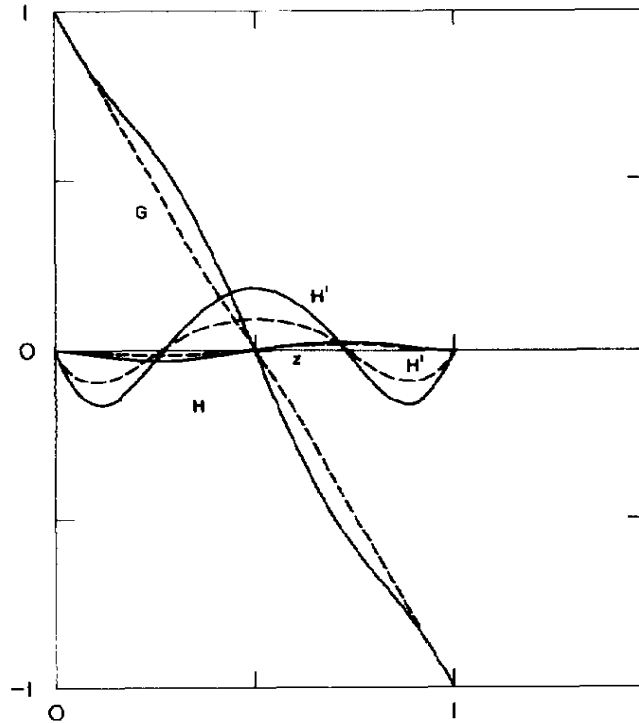


Fig. 11. Comparison of velocity functions for an elastic fluid (—) having $\lambda_1 = 1.25$, $\lambda_2 = 0.21$, $\mu_0 = 0.80$ with those of a slightly elastic non-Newtonian fluid (---) having $\lambda_1 = 0.20$, $\lambda_2 = 0.03$, $\mu_0 = 5.00$; $\Delta z = 0.02$, $\alpha = -1.0$, $\text{Re} = 20$.

$$H < 0 \text{ implies } H_{\text{MAX}} = 0, H_{\text{MIN}} = 1. \quad (36)$$

The equations for P_i can then be written as

$$P_i^k = (1 - 2c) / \left(\frac{S|H|}{\Delta z} + |C_{ii}| \right) \left[X_i^k - \sum_{\substack{j=1 \\ j \neq i}}^8 C_{ij}^k P_j^k \right. \\ \left. + (1 - c) \left(H_{\text{MAX}} \cdot P_i^{k-1} \frac{SH}{\Delta z} - H_{\text{MIN}} \cdot P_i^{k+1} \frac{SH}{\Delta z} \right) \right. \\ \left. + c \left(-H_{\text{MAX}} \cdot P_i^{k+1} \frac{SH}{\Delta z} + H_{\text{MIN}} \cdot P_i^{k-1} \frac{SH}{\Delta z} \right) \right]. \quad (37)$$

To form the successive overrelaxation scheme for Eq. (37), the value of P_i^k is relaxed at each inner iteration, for all the grid values to be calculated, using a relaxation parameter P_ρ . We denote the converged value of the inner iteration loop, by $P_i^{(m)}$, and call it the outer iterative solution, where m represents the number of the outer iteration. This

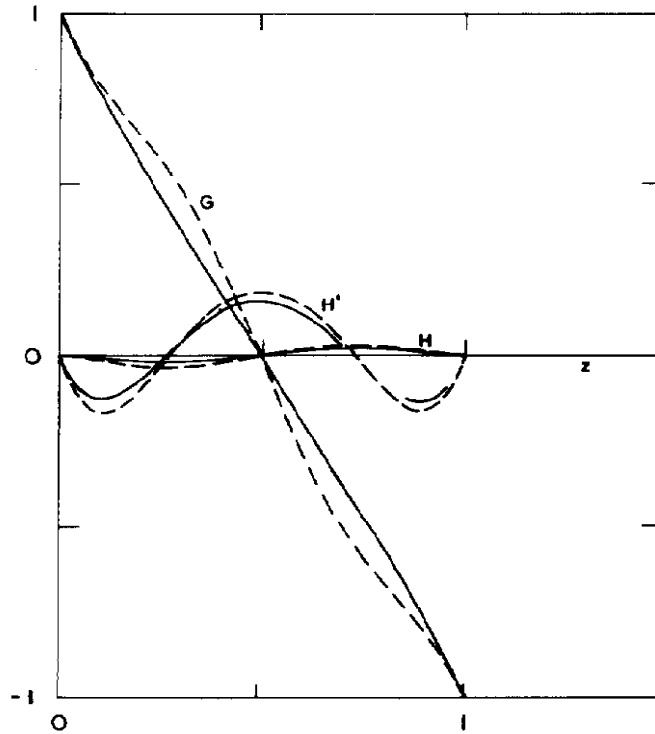


Fig. 12. Comparison of velocity functions for a Newtonian fluid (—) with those of an elastic fluid (---) having $\lambda_1 = 1.25$, $\lambda_2 = 0.21$, $\mu_0 = 0.80$; $\Delta z = 0.02$, $\alpha = -1.0$, $Re = 20$.

outer iterate solution is then smoothed using a smoothing parameter ψ_ρ given by

$$P_i^{(m)} = \psi_\rho \bar{P}_i^{(m)} + (1 - \psi_\rho) \bar{P}_i^{(m-1)}, \tag{38}$$

except at the boundary points where a separate smoothing parameter ψ_{bp} is used.

We say the solution is convergent when a certain convergence criterion is satisfied. For the stresses, this criterion is of the form

$$\left| \left| \frac{P_i^{(m-1)} - P_i^{(m)}}{P_{\max}^{(m)}} \right| \right| < \epsilon_\rho \text{ for all } i. \tag{39}$$

P_{\max} is a norm used for the stresses and in the present case is taken as the maximum value of P in the field at the previous outer iteration. The convergence tests for H , G , and M are similar to the one given above and their specific forms are already given in ref. 1. Thus we shall not list them here.

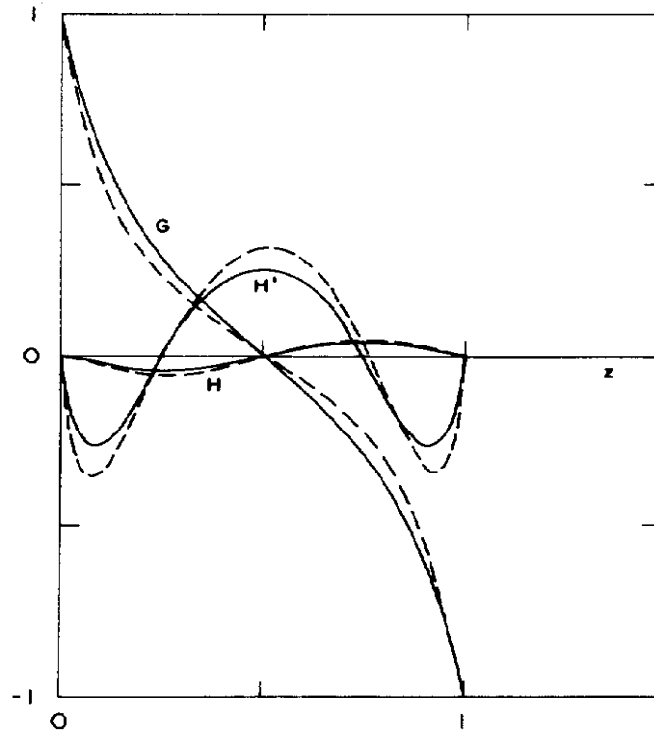


Fig. 13. Comparison of velocity functions for a slightly elastic non-Newtonian fluid (—) having $\lambda_1 = 0.40$, $\lambda_2 = 0.07$, $\mu_0 = 2.50$; with those of a Newtonian fluid (---); $\Delta z = 0.02$, $\alpha = -1.0$, $Re = 100$.

Stability and Convergence

It is known that for Reynolds numbers that are greater than approximately 250, the problem under consideration exhibits multiple solutions.⁸ It has not been our interest in this work to look for such solutions. In fact results presented are only up to $Re = 100$. The highly nonlinear nature of the problem makes the solution scheme rather unstable even in the Newtonian case. Often in such situations iterative solutions require a fairly large number of iterations before convergence is attained, if at all. In the particular problem under consideration, we seek the solutions on a straight line rather than on a two- or three-dimensional grid. This makes it easier to follow the progress of the iterative scheme. As far as the relaxation parameters for the variables H , G , and M are concerned, normally even for the viscoelastic case they can be the same as those for the Newtonian case. The Gauss-Seidel iterative scheme is used for the stresses P_i . However, in the extreme case, i.e., when both the elasticity and the Reynolds number are large, the variable M must be heavily smoothed,

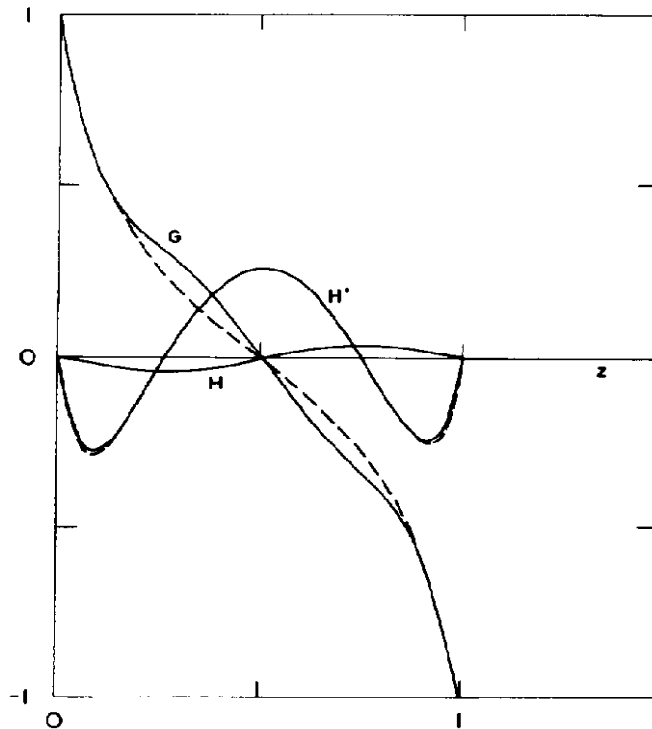


Fig. 14. Comparison of velocity functions for an elastic fluid (—) having $\lambda_1 = 1.00$, $\lambda_2 = 0.17$, $\mu_0 = 1.00$ with those of a slightly elastic non-Newtonian fluid (---) having $\lambda_1 = 0.40$, $\lambda_2 = 0.07$, $\mu_0 = 2.50$; $\Delta z = 0.02$, $\alpha = -1.0$, $Re = 100$.

its inner iteration tolerance increased or even the inner iteration loop done away with altogether.^{17,18}

The magnitude of the tolerance for inner iterative convergence must be chosen carefully. The relative tolerance for each variable must correspond to the relation between the discretization errors of these variables,¹⁹ and also to the relative sensitivities of variables to a change in a given variable. Exact analytical expressions for these relations are not available, but approximate relations could be obtained by considering the discretization schemes and the manner of coupling the variables. It is also possible to obtain some of these relations in real situations by numerical experiments. The shortest way to achieve the convergence seems to depend very much on this choice. The case in which both the disks rotate in opposite directions is much more difficult to handle. Here the convergence could be attained only for fairly restricted values of the material parameters. This is especially true when $Re = 100$. During the iterative process the largest absolute changes take place in the stresses. In fact, they are the last

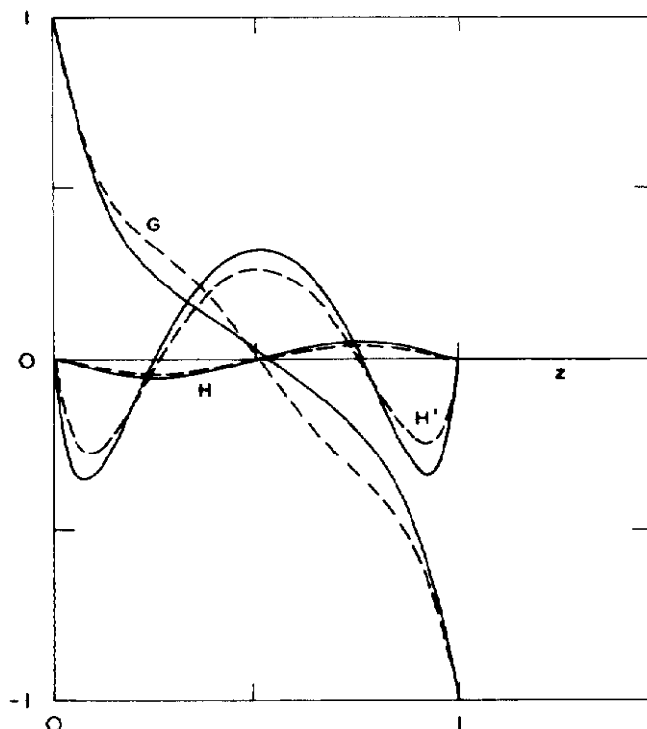


Fig. 15. Comparison of velocity functions for a Newtonian fluid (—) with those of an elastic (---) fluid having $\lambda_1 = 1.0$, $\lambda_2 = 0.17$, $\mu_0 = 1.00$; $\Delta z = 0.02$, $\alpha = -1.0$, $Re = 100$.

to settle down before convergence is attained. Actually convergence is attained in an oscillatory mode at least in some variables. The period of oscillation is not every other iteration but rather a group of such successive iterations. The number of outer iterations in this group decreases as convergence is achieved.

DISCUSSION

We present the results for two different cases, namely (1) $\alpha = 0$, i.e., one disk is held at rest while the other rotates with a constant angular velocity, and (2) $\alpha = -1$, i.e., the disks rotate with constant angular velocities but in opposite directions. For case (1), solutions for two values of Reynolds number are considered, i.e., $Re = 10$ and 100 . On the other hand, for case (2), we consider the solutions for $Re = 10, 20$, and 100 . The reason for this is the desire for inspecting the results in between $Re = 10$ and 100 . This forms a set of six solutions. Each of these six sets, in turn, is comprised of three subsets, these being (a)

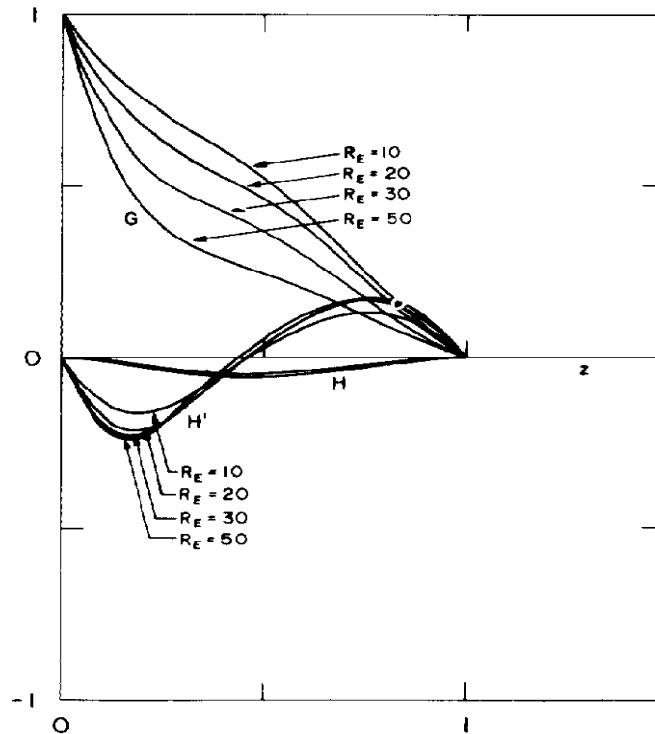


Fig. 16. Changes in G , H , and H' when $Re = 10, 20, 30,$ and 50 for a fixed amount of elasticity and shear thinning. $\Delta z = 0.02, \alpha = 0, \lambda_1 = 1.50, \lambda_2 = 0.25, \mu_0 = 1.00$.

the Newtonian solution, (b) elastic solution with the highest relaxation time λ_1 for which convergence was possible, and (c) the slightly elastic solution which represents the solution for the least relaxation time for which convergence was possible, keeping the product $\lambda_1\mu_0$ constant as λ_1 is decreased. For all elastic solutions, we have chosen $\lambda_1\mu_0 = 1 \text{ s}^2$. The solution with slight elasticity can simulate the non-Newtonian solution in the elastic case¹⁷ when λ_1 is small enough. In the solutions provided, the least λ_1 differs for different solutions. As the influence of λ_1 is not exactly known in each case, the solutions with the least value of λ_1 cannot be considered as the exact non-Newtonian solution with the same shear thinning behavior as the other elastic solutions, since varying degrees of elasticity may be contained therein.

For all of our calculations, we have chosen the grid size $\Delta z = 1/50$ and $\Omega = 1$. Thus, the parameter S is always equal to λ_1 .

Figures 1–6 depict the graphical representation of the velocity functions G , H , and H' for Reynolds number $Re = 10$ and 100 . Choosing $\alpha = 0$, Figure 1 shows the curves of G , H , and H' for a

Newtonian fluid and a non-Newtonian fluid characterized by $\lambda_1 = 0.10$, $\lambda_2 = 0.02$, and $\mu_0 = 1.00$. We note that in this case the curves for two types of fluid are the same. Figure 2 compares the functions G , H , and H' for an elastic fluid characterized by $\lambda_1 = 2.00$, $\lambda_2 = 0.33$, and $\mu_0 = 0.50$ with those for a slightly elastic non-Newtonian fluid. The differences are quite significant. We note that the transverse velocity has a linear variance with z for a slightly elastic fluid while it is not quite so if the fluid is sufficiently elastic. In the central region the transverse velocity is increased because of elasticity, whereas it is decreased near the two disks. The axial velocity suffers only minor changes, owing to elasticity. The point where H' becomes zero is nearer to the rotating disk for an elastic fluid than for a fluid which is only slightly elastic. We observe similar features in Figure 3 in which G , H , and H' are plotted for a Newtonian fluid and an elastic fluid with $\lambda_1 = 2.00$, $\lambda_2 = 0.33$, and $\mu_0 = 0.50$.

Figures 4–6 depict the results for $Re = 100$. In Figure 4, we compare the velocity functions for a Newtonian fluid with those for a slightly elastic non-Newtonian fluid having $\lambda_1 = 0.50$, $\lambda_2 = 0.08$, and $\mu_0 = 2.00$. Figure 6 compares the velocity components for a Newtonian and an elastic liquid characterized by $\lambda_1 = 1.5$, $\lambda_2 = 0.25$, and $\mu_0 = 0.67$. The transverse velocity does not remain linear even for a Newtonian fluid. The elasticity, small or large, decreases the transverse velocity in comparison to a Newtonian fluid. Near the rotating disk, it decreases rapidly within a short distance from this disk, and shows slight increase in the central region before going to zero at the stationary disk. If the fluid has elasticity, the increase in the central region is not so much observable. Looking at the curves for the radial velocity, the boundary layer character of the fluid is more noticeable for Newtonian as well as an elastic fluid, especially near the rotating disk. In both these figures, however, we note that the effect of the elasticity is to decrease the radial velocity near the rotating disk, thereby increasing it at the stationary disk. The point where it vanishes is shifted toward the stationary disk. In Figure 5, comparison is made between G , H , and H' for a non-Newtonian slightly elastic fluid having $\lambda_1 = 1.50$, $\lambda_2 = 0.25$, and $\mu_0 = 0.67$. The general nature of the curves is similar to those in Figures 4 and 6. If the elasticity is high, the transverse velocity is decreased compared with a fluid with slight elasticity. The reverse holds for the axial velocity, which remains always negative for all subcases in which one disk is held at rest. The radial velocity, however, is positive near the

rotating disk because of setting up of a radial outward flow at this disk and is negative near the stationary disk because of a compensatory radial inflow at this disk.

Figures 7–15 depict the corresponding results for the case (2) when $Re = 10, 20,$ and 100 . From Figure 7 in which $G, H,$ and H' are plotted for $Re = 10$, we do not see much difference between a Newtonian and a slightly elastic liquid ($\lambda_1 = 0.20, \lambda_2 = 0.03, \mu_0 = 5.00$) except in the profile for the radial velocity. Comparison is made in Figure 9 between a Newtonian liquid and an elastic liquid ($\lambda_1 = 1.25, \lambda_2 = 0.21, \mu_0 = 0.80$). Figure 8 depicts the differences in the behavior of a slightly elastic liquid (choice of $\lambda_1, \lambda_2, \mu_0$ as in Fig. 7) and an elastic liquid (choice of $\lambda_1, \lambda_2, \mu_0$ as in Fig. 9). We note that if the fluid has elasticity, the transverse velocity is no longer linear. The axial velocity is negative in the lower-half region and is positive in the upper-half region. The radial velocity is positive near the two disks and is negative in the central region. The effects of elasticity are quite clear in Figures 8 and 9. Figures 10–12 demonstrate the results for $Re = 20$ comparing the behavior of a Newtonian, slightly elastic, and an elastic liquid. We note that the flow characteristics are similar to those for $Re = 10$.

Figures 13–15 demonstrate the curves of $G, H,$ and H' for $Re = 100$. We observe some clear differences in the behavior of an elastic liquid in comparison with that of a Newtonian fluid. From Figure 13 we notice that the transverse velocity is no longer linear even for a Newtonian fluid and that the slight elasticity in the liquid ($\lambda_1 = 0.40, \lambda_2 = 0.07, \mu_0 = 2.50$) increases the transverse velocity in the lower-half region and decreases it in the upper-half. As regards the radial velocity, it is smaller than that for the Newtonian fluid near the two counterrotating disks and larger in the central region. The boundary layer character of the flow is also clear from the curves of radial velocity in the neighborhood of the disks. As far as the axial velocity is concerned, the slight elasticity in the liquid increases the axial velocity in the lower-half region and decreases it in the upper-half compared with a Newtonian fluid. Similar features are also observable in Figure 15 in which $G, H,$ and H' are plotted for a Newtonian fluid and a fluid with high elasticity ($\lambda_1 = 1.0, \lambda_2 = 0.17, \mu_0 = 1.0$). From Figure 14, however, the slight or high elasticity in the liquid does not show significant differences except in the transverse velocity, contrary to the similar situations in which one disk is held at rest (see Fig. 5).

Figure 16 is unique in the sense that it shows the changes in G , H , and H' when $Re = 10, 20, 30, 50$ for a fixed amount of elasticity and shear thinning ($\lambda_1 = 1.5, \lambda_2 = 0.25, \mu_0 = 1.00$), if one of the disks is held at rest. We note that as Reynolds number increases, the transverse velocity decreases.

The same is true for the radial velocity but only in the upper-half region. In the lower-half region, however, the radial velocity shows increase with increase in the Reynolds number. The changes in axial velocity are not so significant. We may again point out that although the qualitative characteristics of the flow are similar to those in ref. 1, the fluid model and the numerical procedure utilized in the present study are much superior to that of ref. 1. The convergence is achieved for quite high values of the elastic parameters contrary to the case of a Rivlin-Ericksen fluid where only slight deviations from Newtonian fluid could be considered.

This work was partly completed when the first author was visiting the Department of Chemical Engineering, University of Dortmund, West Germany, on an invitation from Alexander Von Humboldt Foundation. This author also acknowledges the travel support given in January 1979 by Fundação de Amparo à Pesquisa do Estado de São Paulo (FAPESP), Brazil. The authors wish to thank the referees for their valuable suggestions which led to a considerable improvement of the article. Finally, the computing facilities provided by the Twente University of Technology, Enschede, The Netherlands, where a major part of the computations were carried, are gratefully acknowledged.

References

1. R. K. Bhatnagar and J. V. Zago, *Rheol. Acta*, **17**, 557 (1978).
2. K. Stewartson, *Proc. Camb. Philos. Soc.*, **49**, 333 (1953).
3. G. N. Lance and M. H. Rogers, *Proc. R. Soc. London Ser. A*, **266**, 109 (1962).
4. C. E. Pearson, *J. Fluid Mech.*, **73**, 53 (1965).
5. D. Greenspan, *J. Inst. Math. Appl.*, **9**, 370 (1972).
6. G. L. Mellor, P. J. Chapple, and V. K. Stokes, *J. Fluid Mech.*, **31**, 95 (1968).
7. M. Kubicek, M. Holodniok, and V. Hlaváček, *Comp. Fluids*, **4**, 59 (1976).
8. M. Holodniok, M. Kubicek, and V. Hlaváček, *J. Fluid Mech.*, **81**, 689 (1977).
9. M. Kubicek, M. Holodniok, and V. Hlaváček, to appear.
10. A. C. Scrivastava, *Quart. J. Mech. Appl. Math.*, **14**, 353 (1961).
11. R. K. Bhatnagar, *Proc. Ind. Acad. Sci.*, **58**, 279 (1963).
12. R. K. Bhatnagar, *Int. J. Math. Math. Sci.*, **4**, 181 (1981).
13. J. G. Oldroyd, *Proc. R. Soc. London Ser. A*, **200**, 523 (1950).
14. R. S. Varga, *Matrix Iterative Analysis*, Prentice-Hall, Englewood Cliffs, NJ, 1962.
15. D. Greenspan, *Compt. Fluids*, **3**, 69 (1975).
16. M. G. N. Perera and K. Walters, *J. Non-Newton. Fluid Mech.*, **2**, 49 (1977).
17. D. Schultz, *Compt. Fluids*, **7**, 157 (1979).

18. M. G. N. Perera, talk given in school on Numerical Simulation of Viscoelastic Fluid Flow, Brown University, Providence, Rhode Island, November 1979.
19. A. B. Davies, K. Walters, and M. F. Webster, *J. Non-Newt. Fluid Mech.*, **4**, 325 (1979).

Received November 1, 1980

Accepted as revised August 28, 1981